ACS Medicinal Chemistry Letters

pubs.acs.org/acsmedchemlett Letter

Glycans Meet Sphingolipids: Structure-Based Design of Glycan Containing Analogues of a Sphingosine Kinase Inhibitor

Athanasios Papakyriakou,[⊥] Francesca Cencetti,[⊥] Elisa Puliti, Laura Morelli, Jacopo Tricomi, Paola Bruni, Federica Compostella,[*,#] and Barbara Richichi[*,#]

Cite This: *ACS Med. Chem. Lett.* 2020, 11, 913–920 Read Online

ACCESS | Metrics & More | Article Recommendations | Supporting Information

ABSTRACT: Sphingosine 1-phosphate (S1P) is a bioactive lipid mediator associated with diverse homeostatic and signaling roles. Enhanced biosynthesis of S1P, mediated by the sphingosine kinase isozymes (SK1 and SK2), is implicated in several pathophysiological conditions and diseases, including skeletal muscle fibrosis, inflammation, multiple sclerosis, and cancer. Therefore, therapeutic approaches that control S1P production have focused on the development of SK1/2 inhibitors. In this framework, we designed a series of natural monosaccharide-based compounds to enhance anchoring of the known SK1 inhibitor PF-543 at the polar head of the *J-shaped* substrate-binding channel. Herein, we describe the structure-based design and synthesis of new glycan-containing PF-543 analogues and we demonstrate their efficiency in a TGFβ1-induced pro-fibrotic assay.

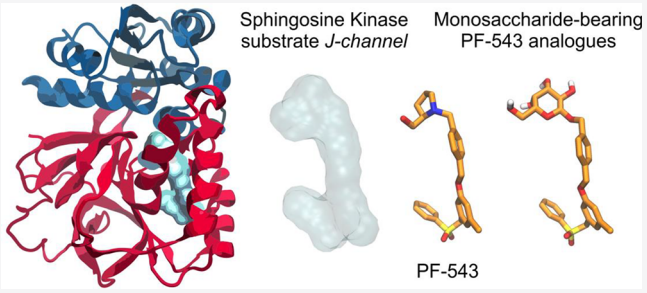

KEYWORDS: *Sphingosine 1-phosphate, skeletal muscle fibrosis, glycan derivatives, molecular modeling, sphingosine kinase 1*

Sphingosine 1-phosphate (**S1P**, Figure 1) has been considered for a long time merely an ultimate metabolite of sphingolipid breakdown. However, the identification of the "inside-out signaling" mechanism associated with S1P production, release, and activity, allowed us to spotlight its key role as a bioactive signaling molecule which regulates many physiological processes as well as pathological ones.[1,2] Intracellular S1P levels are tightly regulated by the crucial balance between its synthesis, mediated by two sphingosine kinase isozymes (SK1 and SK2), and reversible and irreversible degradation catalyzed by S1P phosphatases (SPP1 and SPP2) and S1P lyase, respectively.[3] Specifically, SK1 and SK2 are expressed inside the cells where they show different subcellular localization that endows them with sometimes overlapping otherwise distinct biological effects. SKs catalyze ATP-dependent phosphorylation of sphingosine (**Sph**, Figure 1) inside the cells, and then S1P, besides acting as an intracellular mediator, can be exported in the extracellular *milieu* by means of unspecific ABC family members and specific spinster homologue 2 (SPNS2) transporters, where it interacts with its five specific GPCR receptors designated as S1PR1−5.[4] Thus, SKs are key modulators of the dynamic S1P/sphingosine/ceramide ratio (sphingolipid rheostat model), which in turn affects cellular fate and the balance between cell survival and apoptosis.[5]

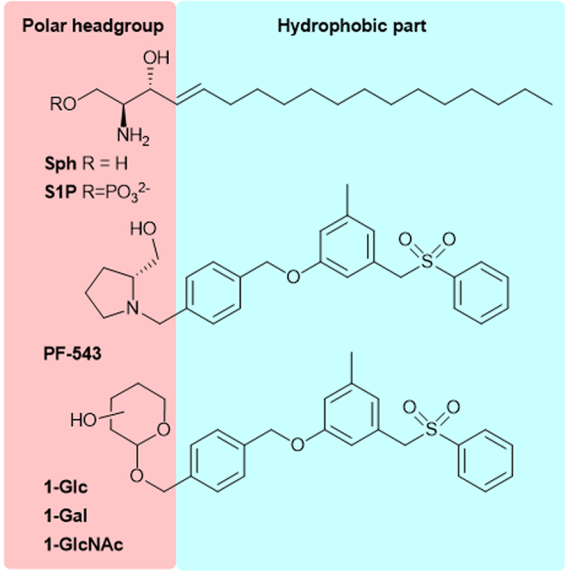

Figure 1. Structures of sphingosine (**Sph**), sphingosine 1-phosphate (**S1P**), **PF-543**, and the new glycoconjugates **1-Glc**, **1-Gal**, and **1-GlcNAc**.

Special Issue: In Memory of Maurizio Botta: His Vision of Medicinal Chemistry

Received: December 30, 2019
Accepted: March 30, 2020
Published: March 30, 2020

https://dx.doi.org/10.1021/acsmedchemlett.9b00665
ACS Med. Chem. Lett. 2020, 11, 913–920

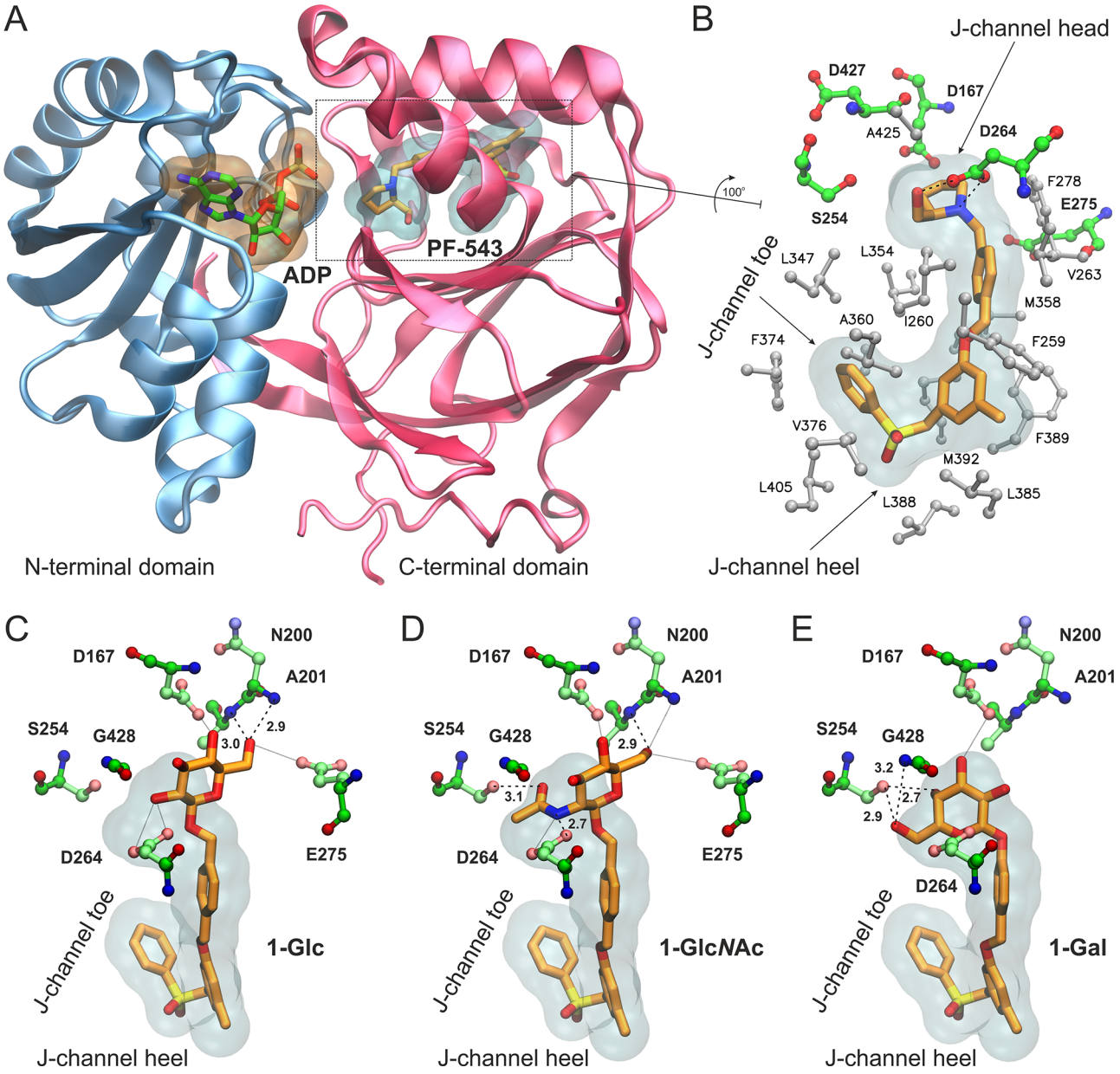

Figure 2. (A) Structure of SK1 with bound ADP and the inhibitor **PF-543** inside the lipid binding channel. SK1 and **PF-543** are taken from the crystal structure with PDB ID 4V24[27] and the nucleotide by superimposing with PDB ID 3VZD.[28] (B) Close-up view of the **Sph**-binding site, "J-channel", illustrating the nonpolar residues (white stick-and-balls) that comprise the foot of the J-channel and the polar residues (green C, blue N, red O) around the polar head of the J-channel. **PF-543** is shown with orange C sticks, and dashed lines indicate the hydrogen bonding interactions with Asp264 (SK1 isoform 2 numbering as in PDB 4V24). Isoform-specific residue changes at the "toe" and "heel" of the J-channel have been proposed to influence inhibitor selectivity for SK1 versus SK2. (C–E) Bound models of the designed analogues **1-Glc** (C), **1-GlcNAc** (D), and **1-Gal** (E) inside the J-channel of SK1. The translucent surfaces indicate the space occupied by **PF-543**, whereas polar residues at the head of the J-channel are shown with ball-and-sticks. Hydrogen bonds are indicated by dashed lines with the heavy-atom distance in Å, whereas putative interactions within 3.5 Å are shown with dotted lines.

The discovery of a link between dysregulation of S1P levels and the onset and progression of several pathological settings (e.g., cancer, autoimmune diseases, atherosclerosis, fibrosis) spotlighted SKs as potential targets for drug discovery.[6,7] In this scenario, we focused on the role of the SK1/S1P3 axis in the onset of skeletal muscle fibrosis, the hallmark of musculoskeletal myopathies. Experimental data showed that the TGFβ1 cytokine-mediated up-regulation of SK1 is responsible for the induction of the fibrotic program in myoblasts.[8] In addition, the remodeling of the S1PR expression pattern occurs and it results in the increased expression of S1P3. Indeed, pharmacological as well as RNA interference approaches targeting SK1 or S1P3 dramatically altered the profibrotic effect induced by TGF1β.[8] Moreover, S1P signaling has been recognized as a new drug target in relapsing-remitting multiple sclerosis. In this framework, a number of SK1 inhibitors have been developed to date.[9−15] However, most of them are still limited by low potency and/or specificity, indicating the need for more performant SK1 inhibitors. Two possible strategies have recently emerged: (i) the targeting of the less conserved SK1 allosteric sites, in order to increase inhibitor affinity and selectivity;[9] (ii) the integration of information from cocrystal structures of SK1 with known

https://dx.doi.org/10.1021/acsmedchemlett.9b00665
ACS Med. Chem. Lett. 2020, 11, 913−920

Scheme 1. Synthesis of 1-Glc, 1-Gal, 1-GlcNAc, and Ac-1-Glc

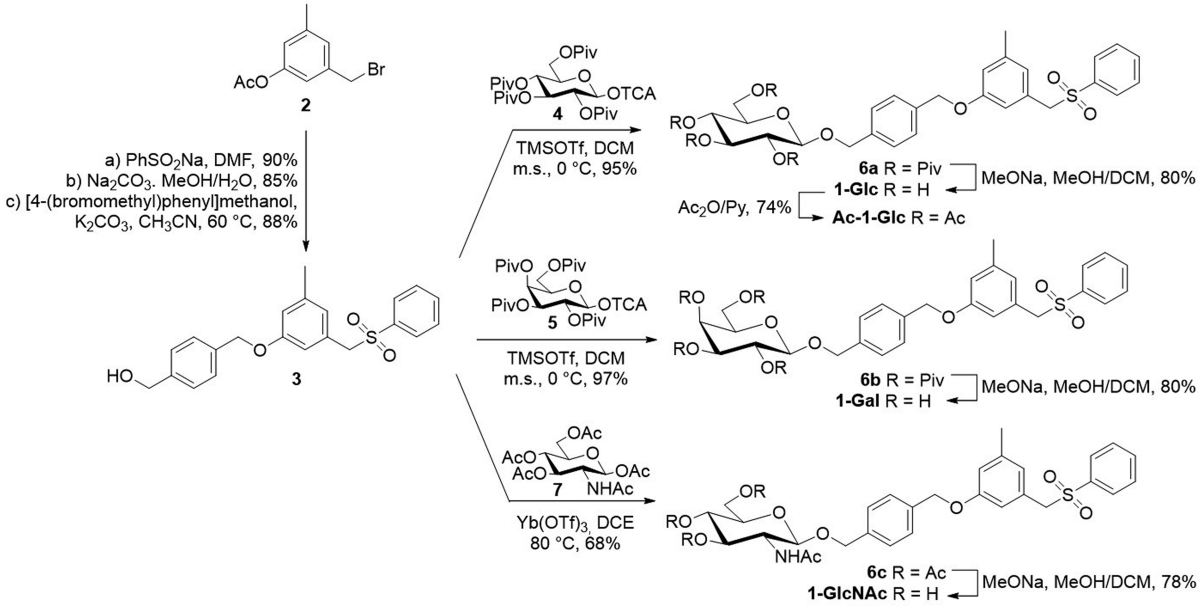

validated inhibitors[14,15] into pharmacophoric models, with the aim to develop more potent inhibitors.

Conjugation of bioactive molecules with carbohydrates has emerged as a straightforward and promising approach to develop glycohybrids as a source of new drug candidates.[16−26] The glycoconjugation approach has been exploited for a wide range of structurally diverse drugs ranging from small organic molecules up to, more recently, macromolecules (e.g., proteins and antibodies).[16,17] This "sweet" functionalization endows researchers to exploit new opportunities to improve both the targeting[21,23,26] and the pharmacokinetic properties of hydrophobic drugs.[18,19] In particular, glycosylation has been exploited as a promising strategy to improve the half-life of therapeutic peptides and proteins (such as somatostatin and opioid drugs, to mention some of them)[18−20] by inducing changes in their conformational structure and consequently in their physiochemical properties. Moreover, the introduction of a glycan moiety has been exploited both to enforce specific tumor-targeting of cytotoxic drugs[21] and to improve the related aqueous solubility of validated proteinases inhibitors.[24,25] The growing scientific interest in this field has inspired us to investigate the use of glycans as the polar headgroup of SK1 inhibitors. To this end, we selected one of the most potent and selective SK1 inhibitor reported so far,[14] **PF-543**, a nonlipid compound bearing 2-hydroxymethylpyrrolidine as a ring-constrained isostere of the aminopropanediol group of the natural substrate (Figure 1). Specifically, it was demonstrated that the pyrrolidine ring provides hydrogen-bonding interactions at the upper part of the cleft of the J-shaped pocket of the enzyme. In this work, we replaced the 2-hydroxymethylpyrrolidine moiety of **PF-543** by selected monosaccharide units (i.e., D-glucose, *N*-acetyl-D-glucosamine, and D-galactose, Figure 1), with the aim to enhance the anchoring of the inhibitor at the *J-shaped* pocked of the enzyme by means of additional interactions provided by the sugar moiety. Herein, we describe the structure-based design and synthesis of monosaccharide-bearing PF-543 analogue SK1 inhibitors, and we provide evidence of their efficiency using a model of TGFβ1-induced skeletal muscle fibrosis.

The design of the monosaccharide-bearing PF-543 analogues was based on the high-resolution crystal structure of SK1 in complex with the inhibitor **PF-543**.[27] SK1 structure consists of an N-terminal domain that binds ATP and a C-terminal domain that harbors the substrate-binding site (Figure 2A). The inhibitor bound inside the highly hydrophobic **Sph**-binding cavity, termed the "J-channel" due to its shape, resembles the bent conformation of a lipid substrate (Figure 2B). The hydroxymethyl-pyrrolidine moiety of **PF-543** occupies the position of a lipid's headgroup next to the γ-phosphate of ATP,[28] and it is anchored by two hydrogen bonds to the carboxylate group of Asp264. Remarkably, no other polar group of **PF-543** was found to participate in hydrogen-bonding interactions within the J-channel.[27] Still, the tight packing of the inhibitor at the hydrophobic pocket occupied by the terminal phenyl group (J-channel toe) and the placement of the sulfonylmethylene group at the heel of the J-channel (Figure 2B) has been proposed to confer the selectivity of **PF-543** for SK1 (IC_{50} = 25 nM) versus SK2 (IC_{50} > 5,000 nM).[11] Now, considering that a glycan moiety at the head of the J-channel would offer the potential for additional polar interactions, we retained the hydrophobic moiety of **PF-543**, which could be fine-tuned at a later stage to modulate the selectivity profile for SK1/SK2, as demonstrated recently.[11]

Indeed, our molecular docking calculations suggest that a β-D-glucopyranose moiety can be accommodated inside the **Sph**-binding site of SK1 without affecting the conformation of the hydrophobic moiety of **PF-543** at the J-channel (Figure 2C). The selected bound conformation of **1-Glc** exhibits two hydrogen bonds between 6-OH and the backbone NH groups of Asn200 and Ala201. In addition, 2-OH of **1-Glc** is within hydrogen-bonding distance from the side-chain of Asp264, albeit the geometry is not ideal (Figure 2C). This is also the case for the 6-OH of **1-Glc** and the distal Glu275, as well as the 4-OH of **1-Glc** and the carboxylate group of Asp167, which is located at the N-terminal domain of SK1. The *N*-acetyl glucosamine derivative **1-GlcNAc** is predicted to interact with SK1 via hydrogen bonds of its amide NH with the carboxylate group of Asp264 and its acetyl C═O with the hydroxyl group of Ser254

https://dx.doi.org/10.1021/acsmedchemlett.9b00665
ACS Med. Chem. Lett. 2020, 11, 913−920

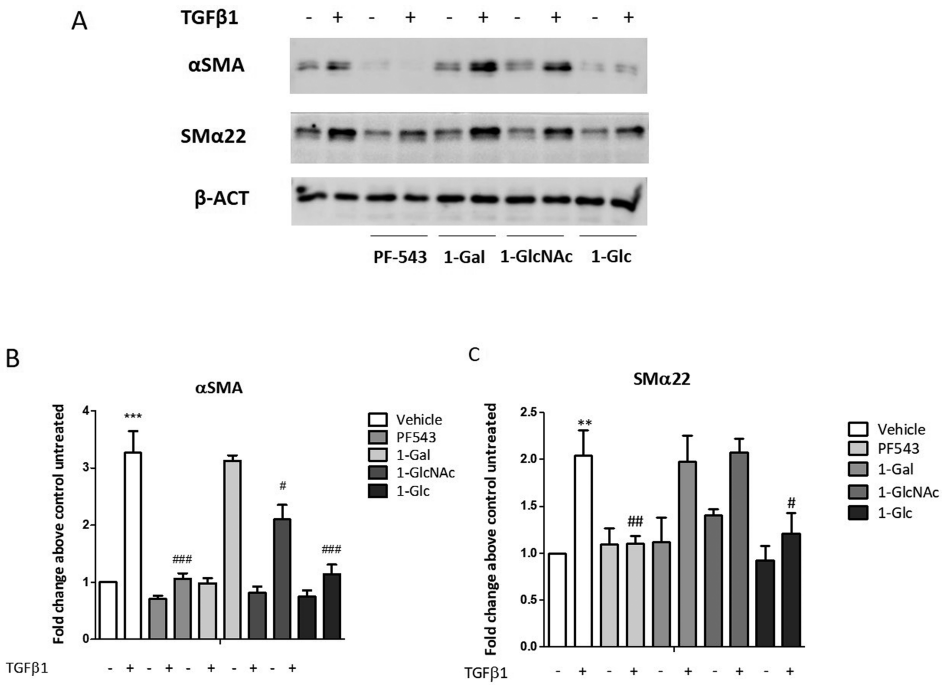

Figure 3. Effect of glycoconjugates **1-Glc**, **1-Gal**, and **1-GlcNAc** compared to **PF-543** on TGFβ1-induced fibrosis marker expression in murine myoblasts. C2C12 myoblasts were seeded to 80% confluence and challenged with 5.0 ng/mL TGFβ1, **PF-543**, **1-Gal**, **1-GalNAc**, and **1-Glc** (30 min, 10 μM). (A) The expression of protein markers which expression correlates with muscle fibrosis, has been evaluated by Western blot analysis, using specific anti-α-SMA and anti-SMα22. A representative blot is shown among three independent experiments with analogous results. (B and C) Densitometric analysis was performed of three independent experiments, and data, normalized to β-actin expression, were reported as mean ± SD of fold change above control untreated. The effect of TGFβ1 on fibrosis marker expression was significant by student *t* test. $^{**}P < 0.01$. $^{***}P < 0.001$. The effect of pharmacological inhibition of SK1 on TGFβ1 induced fibrosis marker expression was significant by two-way ANOVA followed by Bonferroni *posthoc* test. #$P < 0.05$, ##$P < 0.01$, ###$P < 0.001$.

(Figure 2D). Notably, Ser254 has been shown to interact with the polar head of the substrate[28] but not with **PF-543**.[27] An additional H-bond could be formed by the 6-OH of **1-GlcNAc** and the amide group of Ala201, including potential interactions with the side-chains of Asp167 and Glu275, similar to **1-Glc**. With the aim to investigate the role of the sugar stereochemistry at position C-4, we also employed β-D-galactose as a polar head. Our calculations suggest that the 6-OH and 4-OH of **1-Gal** could be engaged in hydrogen bonding interactions with the hydroxyl group of Ser254 and the amide NH group of Gly428 (Figure 2E). The 3-OH group of **1-Gal** is also within hydrogen bonding distance from the side-chain of Asp167; however, at this bound pose there is no potential for direct interaction with Ala201, Asp264, or Glu275. Taken together, our analysis indicates that our design strategy is expected to yield analogues bearing the hydrophobic moiety of **PF-543** that can be well accommodated within the J-channel of SK1. The introduction of a sugar moiety at the J-channel head endows the potential for additional hydrogen-bonding interactions with polar residues of SK1.

Compounds **1-Glc**, **1-Gal**, and **1-GlcNAc** were synthesized following a convergent approach (Scheme 1). The hydrophobic scaffold **3** was prepared through an optimized procedure[29] starting from commercially available 3-(bromomethyl)-5-methylphenyl acetate **2** (see SI). Compound **3** was then used as the acceptor in the glycosylation reactions to give the target compounds **1** (Scheme 1). In particular, the glucosyl **1-Glc** and galactosyl **1-Gal** derivatives were obtained through a glycosylation reaction between the per-pivaloylated glycosyl trichloroacetimidate donors (**4**[30] and **5**,[31] respectively) and acceptor **3**, followed by acyl deprotection through Zèmplen transesterification. In both cases the glycosylation reactions proceed in high yield and complete stereoselectivity, and compounds **6a** and **6b** were recovered as pure β-glycosides (95% and 97% yield, respectively). A different strategy was used to prepare the *N*-acetyl D-glucosamine (GlcNAc) derivative **1-GlcNAc** (Scheme 1). In this case, commercially available D-glucosamine pentaacetate **7** was reacted at high temperature with glycosyl acceptor **3** using ytterbium triflate as the catalyst to give **6c** in satisfactory yield.[32] Zemplén deacetylation of **6c** with sodium methoxide in methanol gave efficiently (78%) the GlcNAc containing inhibitor **1-GlcNAc**.

TGF-β is involved in the regulation of skeletal muscle fibrosis as it was shown to be a potent inducer of myoblasts into myofibroblasts transdifferentiation,[33] with a molecular mechanism relying on cytokine-mediated SK1 activation. On this basis, the ability of the new glycoconjugates to interfere with TGFβ1-induced fibrosis in C2C12 myoblasts was evaluated. **PF-543** was used as reference control in this study at the concentration of 10 μM according with data in the literature.[34−36] Cells were incubated with 10 μM of the inhibitors (*e.g.* **PF-543**, **1-Gal**, **1-GlcNAc**, and **1-Glc**) for 30 min before the addition of the 5.0 ng/mL solution of TGFβ1. The expression of protein markers that correlate with muscle fibrosis was evaluated by Western blot analysis using specific anti-α-SMA and anti-SMα22. Total cell lysates were subjected to Western blot analysis to measure the relative content of fibrosis markers. In agreement with previous data,[8] 48 h TGFβ1 treatment induced the expression of fibrosis markers (Figure 3). Subsequently, treatment with **PF-543** (10 μM) resulted in abrogation of the α-SMA expression induced by

https://dx.doi.org/10.1021/acsmedchemlett.9b00665
ACS Med. Chem. Lett. 2020, 11, 913−920

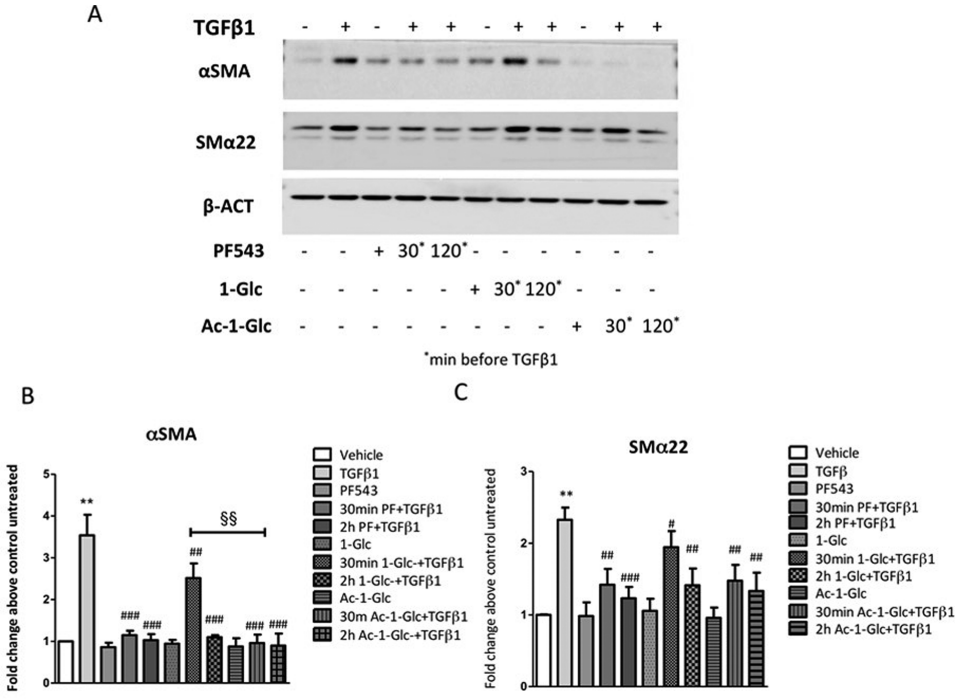

Figure 4. Effect of **1-Glc** and **Ac-1-Glc** compared to **PF-543** in TGFβ1-induced fibrosis marker expression in murine myoblasts. C2C12 myoblasts were seeded to 80% confluence and treated with 5.0 ng/mL TGFβ1, **PF-543**, **1-Glc**, and **Ac-1-Glc** (30 min, 120 min). (A) The expression of protein markers, which expression correlates with muscle fibrosis, has been evaluated by Western blot analysis, using specific anti-α-SMA and anti-SMα22. A representative blot is shown among three independent experiments with analogous results. (B and C) Densitometric analysis was performed of three independent experiments and data, normalized to β-actin expression, were reported as mean ± SD of fold change above control untreated. The effect of pharmacological inhibition of SK1 on TGFβ1 induced fibrosis marker expression was significant by two-way ANOVA followed by Bonferroni *posthoc* test. #$P < 0.05$, ##$P < 0.01$, ###$P < 0.001$. The effect of pharmacological inhibition of SK1 by 30 min **Ac-1-Glc** compared to **1-Glc** on TGFβ1 induced αSMA expression was significant by two-way ANOVA followed by Bonferroni *posthoc* test. §§$P < 0.01$.

TGFβ1 whereas the expression of SMα22 was significantly affected (Figure 3). The three glycoconjugates (**1-Glc**, **1-Gal** and **1-GlcNAc**) displayed a variable effect according with the glycan residue (Figure 3). Both the α-SMA and SMα22 expression induced by TGFβ1 were not affected by **1-Gal**, while **1-GlcNAc** displayed a partial inhibition of α-SMA expression. Notably, **1-Glc** significantly affected both the α-SMA and SMα22 expression induced by TGFβ1, an effect comparable to that displayed by **PF-543** (Figure 3).

Considering that acetylation of the hydroxyl groups of glycans has been proved to be an efficient approach to promote transit of glycan containing molecules across the plasma membrane,[37] we also sought to investigate the activity of the per-acetylated derivative of **1-Glc**, **Ac-1-Glc** (Scheme 1). Therefore, a dose dependence of **1-Glc** and **Ac-1-Glc** compared to the parental drug **PF-543** on TGFβ1-induced fibrosis of murine myoblasts was performed in order to define the bioactive concentration. Western blot data (see SI, Figure S1) confirmed that 10 μM resulted in the most effective concentration on affecting the expression of both α-SMA and SMα22. Then, Western blot analysis was performed to detect the relative expression of fibrosis markers induced by TGFβ1 after 30 min and 2 h treatments with **1-Glc**, **Ac-1-Glc**, and **PF-543** as control (Figure 4). The TGFβ1-induced α-SMA expression was completely abrogated by **Ac-1-Glc** after 30 min, whereas the expression of SMα22 was significantly decreased after 2 h treatment (Figure 4). Notably, the effect of pharmacological inhibition of TGFβ1 induced α-SMA expression after 30 min **Ac-1-Glc** treatment was significantly higher compared to **1-Glc** (two-way ANOVA followed by Bonferroni *posthoc* test, §§$P < 0.01$, Figure 4), supporting our rationale.

Laser scanning confocal microscopy was employed to outline the distribution of fibrosis markers that are functional cytoskeletal proteins, whose expression can be analyzed to follow the onset and progression of skeletal muscle fibrosis. Confocal immunofluorescence analysis revealed an enhanced expression of αSMA in C2C12 cells treated with 5.0 ng/mL TGFβ1 for 48 h, which resulted mainly localized within F-actin microfilaments (Figure 5). In agreement with previous results, the treatment with **PF-543** as well as **1-Glc** and **Ac-1-Glc** (10 μM) completely prevented the cytokine-induced expression of αSMA (Figure 5).

It has been extensively demonstrated that TGF-β family members are implicated in the regulation of myogenic differentiation as they were shown to be potent inhibitors of myoblasts differentiation. Exogenous TGFβ1 was shown to prevent features of skeletal muscle differentiation, such as fusion and myotube formation, in different cultured cell lines *in vitro*,[38,39] and the molecular mechanism at least in part relies on SK1 activation by the cytokine.[8] For this reason, **1-Glc** and **Ac-1-Glc** conjugates were assayed for the effect on TGFβ1-mediated myoblast differentiation compared to **PF-543**. For this purpose, Western blot analysis was performed to measure the relative expression of caveolin-3 (Cav-3) by TGFβ1 after 30 min, 1 h, and 2 h incubation with **PF-543**, **1-Glc**, and **Ac-1-Glc** glycoconjugates. Data (see SI, Figure S2) showed that, as expected, TGFβ1 decreases skeletal muscle differentiation whereas this effect was significantly reverted by both **1-Glc**

https://dx.doi.org/10.1021/acsmedchemlett.9b00665
ACS Med. Chem. Lett. 2020, 11, 913−920

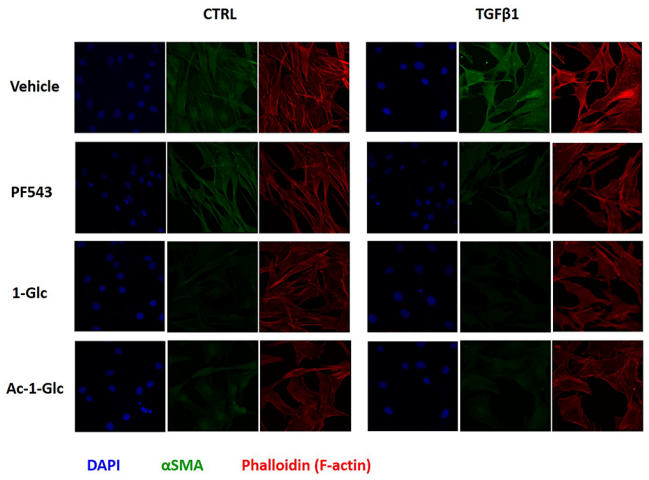

Figure 5. Confocal immunofluorescence analysis was performed in 24 h serum-starved C2C12 cells that were treated with 5.0 ng/mL TGFβ1, after a 2 h of incubation with **PF-543**, **1-Glc**, and **Ac-1-Glc**. Anti-αSMA primary antibody and fluorescein-conjugated antimouse secondary antibody were used. DAPI was added to label nuclei and rhodamine-phalloidin as high-affinity F-actin probe in order to trace cytoskeletal microfilaments. The immunofluorescence images shown are representative of six fields for each condition.

and **Ac-1-Glc** and it was almost completely abolished at 2 h of incubation.

Taken together our findings suggest that the glucose-bearing derivative and in particular its acetylated form **Ac-1-Glc** is the most active compound, as it completely abrogates the TGFβ1 induced expression of a key fibrosis marker. Although additional structural and biochemical information is required, we can hypothesize that the lower potency of **1-Gal** compared to **1-Glc** and **1-GlcNAc** is due to the lack of interaction with the side-chain of Asp264 (Figure 2C–E), a key residue that has been shown to provide the only hydrogen-bonding interactions of **PF-543** within the J-channel of SK1. In conclusion, our work demonstrates that the use of natural monosaccharides as the polar headgroup of known SK inhibitors offers the potential to develop a new class of signaling molecules that regulate the expression of fibrosis markers. The biological effects of the new PF-543 analogues on TGFβ1-profibrotic effects in myoblasts suggest a possible interaction and inhibition of the catalytic site of SK1. However, further studies (e.g., binding data and further biochemical and pharmacological characterizations) are needed to corroborate this hypothesis. Finally, considering the sugar heterogeneity in terms of stereochemistry and availability of functional groups, our findings suggest that glycans can be employed as an additional tool to explore the pharmacological profile of modulators of the sphingolipid rheostat model.

EXPERIMENTAL SECTION

General. Standard laboratory procedures were followed to carry out the reactions and to prepare dry solvents. Optical rotations were measured with a PerkinElmer 241 polarimeter at 20 °C. ^{1}H and ^{13}C NMR spectra were recorded with a Bruker AVANCE-500 spectrometer at a sample temperature of 298 K. High-resolution mass spectra were collected by electrospray ionization (ESI) spectroscopy on a QTof SYNAPT G2Si Mass Spectrometer.

4-[(3-Methyl-5-(phenylsulfonylmethyl)-phenoxy)methyl]-phenylmethyl β-D-Glucopyranoside (1-Glc). To a stirred solution of compound **6a** (0.25 g, 0.028 mmol) in DCM (0.5 mL) was added sodium methoxide in methanol (0.1 M solution, 0.56 mL). The reaction was stirred at room temperature, and further portions of sodium methoxide (0.1 M solution, 0.30 mL) were added every 12 h. After 24 h the reaction mixture was neutralized with an ion-exchange resin (Dowex 50 × 8, H^+ form), filtered, and concentrated. The crude product was subjected to flash chromatography (DCM/MeOH, 9:1) to give pure **1-Glc** (0.012 g, 80%) as an amorphous white solid. $[\alpha]_D^{20}$ = −32.0 (c = 0.5 in chloroform). ^{1}H NMR ($CDCl_3/CD_3OD$, 2:1): δ = 7.68–7.62 (m, 3H, arom.), 7.53–7.47 (m, 2H, arom.), 7.44–7.39 (m, 2H, arom.), 7.37–7.33 (m, 2H, arom.), 6.74 (*br* s, 1H, arom.), 6.49 (*br* s, 1H, arom.), 6.48 (*br* s, 1H, arom.), 4.96–4.92 (m, 3H, OC*Ha*Hb and CH_2SO_2), 4.68 (d, 1H, J = 11.8 Hz, OCHa*Hb*), 4.38 (d, 1H, $J_{1,2}$ = 7.7 Hz, H-1), 4.28 (s, 2H, $PhCH_2O$), 3.88 (dd, 1H, $J_{5,6a}$ = 2.7 Hz, $J_{6a,6b}$ = 12.0 Hz, H-6a), 3.74 (dd, 1H, $J_{5,6b}$ = 5.3 Hz, $J_{6a,6b}$ = 12.0 Hz, H-6b), 3.43–3.35 (m, 2H, H-3,4), 3.35–3.26 (m, 2H, H-2,5), 2.20 (s, 3H, CH_3). ^{13}C NMR ($CDCl_3/CD_3OD$, 2:1): δ = 158.6, 139.7, 137.6, 137.2, 136.4, 133.8, 128.9–127.4 (9C), 124.4, 116.4, 114.0, 102.0 (C-1), 76.6, 76.2 (C-5), 73.6 (C-2), 70.6 (OCH_2), 70.3, 69.6 (CH_2SO_2), 62.6 ($PhCH_2O$), 61.7 (C-6), 20.9 (CH_3). HRMS (ESI): m/z calcd for $C_{28}H_{32}O_9NaS$ 567.1665 $[M + Na]^+$, found 567.1665.

ASSOCIATED CONTENT

Supporting Information

The Supporting Information is available free of charge at https://pubs.acs.org/doi/10.1021/acsmedchemlett.9b00665.

Figures **S1** and **S2**. Synthetic procedures for the synthesis of compounds **3, 6a–c**, **1-Gal**, **1-GlcNAc**, and **Ac-1-Glc**. Computational and biological methods. ^{1}H and ^{13}C spectra of new compounds. (PDF)

Coordinate file of the SK1 bound with **1-Glc** model (PDB)

Coordinate file of the SK1 bound with **1-GlcNAc** model (PDB)

Coordinate file of the SK1 bound with **1-Gal** model (PDB)

AUTHOR INFORMATION

Corresponding Authors

Federica Compostella – *Department of Medical Biotechnology and Translational Medicine, University of Milan, 20133 Milano, Italy*; orcid.org/0000-0003-4721-0358; Email: federica.compostella@unimi.it

Barbara Richichi – *Department of Chemistry "Ugo Schiff", University of Florence, 50019 Sesto Fiorentino, FI, Italy*; orcid.org/0000-0001-7093-9513; Email: barbara.richichi@unifi.it

Authors

Athanasios Papakyriakou – *Institute of Biosciences & Applications, National Centre for Scientific Research "Demokritos", GR-15341 Agia Paraskevi, Athens, Greece*; orcid.org/0000-0003-3931-6232

Francesca Cencetti – *Department of Experimental and Clinical Biomedical Sciences, University of Florence, 50134 Firenze, Italy*

Elisa Puliti – *Department of Experimental and Clinical Biomedical Sciences, University of Florence, 50134 Firenze, Italy*

Laura Morelli – *Department of Medical Biotechnology and Translational Medicine, University of Milan, 20133 Milano, Italy*

Jacopo Tricomi – *Department of Chemistry "Ugo Schiff", University of Florence, 50019 Sesto Fiorentino, FI, Italy*

Paola Bruni – *Department of Experimental and Clinical Biomedical Sciences, University of Florence, 50134 Firenze, Italy*

Complete contact information is available at: https://pubs.acs.org/10.1021/acsmedchemlett.9b00665

https://dx.doi.org/10.1021/acsmedchemlett.9b00665
ACS Med. Chem. Lett. 2020, 11, 913–920

Author Contributions
[⊥]A.P. and F.Ce. contributed equally to this work.

Author Contributions
[#]F.Co. and B.R. are colast and cocorresponding authors.

Funding
We thank Fondazione Cassa di Risparmio di Firenze (project #24081: Sviluppo di modulatori dei recettori per la sfingosina 1-fosfato: verso il controllo dell'atrofia muscolo scheletrica). B.R., F.C., J.T., and L.M. thank COST Action CA18013. B.R., J.T., F.Ce. and P.B. thank MIUR-Italy ("Progetto Dipartimenti di Eccellenza 2018−2022" allocated to Department of Chemistry "Ugo Schiff" and to the Department of Experimental and Clinical Biomedical Sciences "Mario Serio").

Notes
The authors declare no competing financial interest.

■ ACKNOWLEDGMENTS

F.Co. and L.M. thank "Centro Interdipartimentale Grandi Apparecchiature (C.I.G.A.)" for HRMS analyses.

■ ABBREVIATIONS

Glc, D-glucose; Gal, D-galactose; GlcNAc, *N*-acetyl-D-glucosamine; Sph, sphingosine; S1P, sphingosine 1-phosphate; SK, sphingosine kinase; SPNS2, specific spinster homologue 2; SPP, sphingosine 1-phosphate phosphatases

■ REFERENCES

(1) Takabe, K.; Paugh, S. W.; Milstien, S.; Spiegel, S. "Inside-out" signaling of sphingosine-1-phosphate: therapeutic targets. *Pharmacol. Rev.* **2008**, *60* (2), 181−195.
(2) Cartier, A.; Hla, T. Sphingosine 1-phosphate: Lipid signaling in pathology and therapy. *Science* **2019**, *366* (6463), eaar5551
(3) Ksiazek, M.; Chacinska, M.; Chabowski, A.; Baranowski, M. Sources, metabolism, and regulation of circulating sphingosine-1-phosphate. *J. Lipid Res.* **2015**, *56* (7), 1271−1281.
(4) Rosen, H.; Goetzl, E. J. Sphingosine 1-phosphate and its receptors: an autocrine and paracrine network. *Nat. Rev. Immunol.* **2005**, *5* (7), 560−570.
(5) Newton, J.; Lima, S.; Maceyka, M.; Spiegel, S. Revisiting the sphingolipid rheostat: Evolving concepts in cancer therapy. *Exp. Cell Res.* **2015**, *333* (2), 195−200.
(6) Sukocheva, O. A.; Furuya, H.; Ng, M. L.; Friedemann, M.; Menschikowski, M.; Tarasov, V. V.; Chubarev, V. N.; Klochkov, S. G.; Neganova, M. E.; Mangoni, A. A.; Aliev, G.; Bishayee, A. Sphingosine kinase and sphingosine-1-phosphate receptor signaling pathway in inflammatory gastrointestinal disease and cancers: A novel therapeutic target. *Pharmacol. Ther.* **2020**, *207*, 107464.
(7) Khan, F. I.; Lai, D.; Anwer, R.; Azim, I.; Khan, M. K. A. Identifying novel sphingosine kinase 1 inhibitors as therapeutics against breast cancer. *J. Enzyme Inhib. Med. Chem.* **2020**, *35*, 172−186.
(8) Cencetti, F.; Bernacchioni, C.; Nincheri, P.; Donati, C.; Bruni, P. Transforming growth factor-beta1 induces transdifferentiation of myoblasts into myofibroblasts via up-regulation of sphingosine kinase-1/S1P3 axis. *Mol. Biol. Cell* **2010**, *21* (6), 1111−1124.
(9) Bayraktar, O.; Ozkirimli, E.; Ulgen, K. Sphingosine kinase 1 (SK1) allosteric inhibitors that target the dimerization site. *Comput. Biol. Chem.* **2017**, *69*, 64−76.
(10) Cao, M.; Ji, C.; Zhou, Y.; Huang, W.; Ni, W.; Tong, X.; Wei, J. F. Sphingosine kinase inhibitors: A patent review. *Int. J. Mol. Med.* **2018**, *41*, 2450−2460.
(11) Adams, D. R.; Tawati, S.; Berretta, G.; Rivas, P. L.; Baiget, J.; Jiang, Z.; Alsfouk, A.; Mackay, S. P.; Pyne, N. J.; Pyne, S. Topographical Mapping of Isoform-Selectivity Determinants for J-Channel-Binding Inhibitors of Sphingosine Kinases 1 and 2. *J. Med. Chem.* **2019**, *62*, 3658−3676.
(12) Magli, E.; Corvino, A.; Fiorino, F.; Frecentese, F.; Perissutti, E.; Saccone, I.; Santagada, V.; Caliendo, G.; Severino, B. Design of Sphingosine Kinases Inhibitors: Challenges and Recent Developments. *Curr. Pharm. Des.* **2019**, *25*, 956−968.
(13) Vettorazzi, M.; Angelina, E.; Lima, S.; Gonec, T.; Otevrel, J.; Marvanova, P.; Padrtova, T.; Mokry, P.; Bobal, P.; Acosta, L. M.; Palma, A.; Cobo, J.; Bobalova, J.; Csollei, J.; Malik, I.; Alvarez, S.; Spiegel, S.; Jampilek, J.; Enriz, R. D. An integrative study to identify novel scaffolds for sphingosine kinase 1 inhibitors. *Eur. J. Med. Chem.* **2017**, *139*, 461−481.
(14) Schnute, M. E.; McReynolds, M. D.; Kasten, T.; Yates, M.; Jerome, G.; Rains, J. W.; Hall, T.; Chrencik, J.; Kraus, M.; Cronin, C. N.; Saabye, M.; Highkin, M. K.; Broadus, R.; Ogawa, S.; Cukyne, K.; Zawadzke, L. E.; Peterkin, V.; Iyanar, K.; Scholten, J. A.; Wendling, J.; Fujiwara, H.; Nemirovskiy, O.; Wittwer, A. J.; Nagiec, M. M. Modulation of cellular S1P levels with a novel, potent and specific inhibitor of sphingosine kinase-1. *Biochem. J.* **2012**, *444* (1), 79−88.
(15) Gustin, D. J.; Li, Y.; Brown, M. L.; Min, X.; Schmitt, M. J.; Wanska, M.; Wang, X.; Connors, R.; Johnstone, S.; Cardozo, M.; Cheng, A. C.; Jeffries, S.; Franks, B.; Li, S.; Shen, S.; Wong, M.; Wesche, H.; Xu, G.; Carlson, T. J.; Plant, M.; Morgenstern, K.; Rex, K.; Schmitt, J.; Coxon, A.; Walker, N.; Kayser, F.; Wang, Z. Structure guided design of a series of sphingosine kinase (SphK) inhibitors. *Bioorg. Med. Chem. Lett.* **2013**, *23* (16), 4608−4616.
(16) Solà, R. J.; Griebenow, K. Glycosylation of Therapeuic Proteins: an effective strategy to optimize efficacy. *BioDrugs* **2010**, *24*, 9−21.
(17) Moradi, S. V.; Hussein, W. M.; Varamini, P.; Simerska, P.; Toth, I. Glycosylation, an effective synthetic strategy to improve the bioavailability of therapeutic peptides. *Chem. Sci.* **2016**, *7* (4), 2492−2500.
(18) Egleton, R. D.; Mitchell, S. A.; Huber, J. D.; Janders, J.; Stropova, D.; Polt, R.; Yamamura, H. I.; Hruby, V. J.; Davis, T. P. Improved bioavailability to the brain of glycosylated Met-enkephalin analogs. *Brain Res.* **2000**, *881* (1), 37−46.
(19) Witt, K. A.; Gillespie, T. J.; Huber, J. D.; Egleton, R. D.; Davis, T. P. Peptide drug modifications to enhance bioavailability and blood-brain barrier permeability. *Peptides* **2001**, *22* (12), 2329−2343.
(20) Albert, R.; Marbach, P.; Bauer, W.; Briner, U.; Fricker, G.; Bruns, C.; Pless, J. SDZ CO 611: a highly potent glycated analog of somatostatin with improved oral activity. *Life Sci.* **1993**, *53* (6), 517−25.
(21) Liu, R.; Fu, Z.; Zhao, M.; Gao, X.; Li, H.; Mi, Q.; Liu, P.; Yang, J.; Yao, Z.; Gao, Q. GLUT1-mediated selective tumor targeting with fluorine containing platinum(II) glycoconjugates. *Oncotarget* **2017**, *8*, 39476−39496.
(22) Fisher, J. F.; Harrison, A. W.; Bundy, G. L.; Wilkinson, K. F.; Rush, B. D.; Ruwart, M. J. Peptide to glycopeptide: glycosylated oligopeptide renin inhibitors with attenuated in vivo clearance properties. *J. Med. Chem.* **1991**, *34* (10), 3140−3.
(23) Chen, X.; Hui, L.; Foster, D. A.; Drain, C. M. Efficient synthesis and photodynamic activity of porphyrin-saccharide conjugates: targeting and incapacitating cancer cells. *Biochemistry* **2004**, *43* (34), 10918−10929.
(24) Fragai, M.; Nativi, C.; Richichi, B.; Venturi, C. Design in silico, synthesis and binding evaluation of a carbohydrate-based scaffold for structurally novel inhibitors of matrix metalloproteinases. *ChemBioChem* **2005**, *6* (8), 1345−1349.
(25) Nuti, E.; Cuffaro, D.; D'Andrea, F.; Rosalia, L.; Tepshi, L.; Fabbi, M.; Carbotti, G.; Ferrini, S.; Santamaria, S.; Camodeca, C.; Ciccone, L.; Orlandini, E.; Nencetti, S.; Stura, E. A.; Dive, V.; Rossello, A. Sugar-Based Arylsulfonamide Carboxylates as Selective and Water-Soluble Matrix Metalloproteinase-12 Inhibitors. *ChemMedChem* **2016**, *11*, 1626−1637.
(26) Christie, M. P.; Simerska, P.; Jen, F. E.; Hussein, W. M.; Rawi, M. F.; Hartley-Tassell, L. E.; Day, C. J.; Jennings, M. P.; Toth, I. A drug delivery strategy: binding enkephalin to asialoglycoprotein receptor by enzymatic galactosylation. *PLoS One* **2014**, *9* (4), No. e95024.

(27) Wang, J.; Knapp, S.; Pyne, N. J.; Pyne, S.; Elkins, J. M. Crystal Structure of Sphingosine Kinase 1 with PF-543. *ACS Med. Chem. Lett.* **2014**, *5* (12), 1329−1333.
(28) Wang, Z.; Min, X.; Xiao, S. H.; Johnstone, S.; Romanow, W.; Meininger, D.; Xu, H.; Liu, J.; Dai, J.; An, S.; Thibault, S.; Walker, N. Molecular basis of sphingosine kinase 1 substrate recognition and catalysis. *Structure* **2013**, *21* (5), 798−809.
(29) Schnute, M. E.; McReynolds, M. D.; Carroll, J.; Chrencik, J.; Highkin, M. K.; Iyanar, K.; Jerome, G.; Rains, J. W.; Saabye, M.; Scholten, J. A.; Yates, M.; Nagiec, M. M. Discovery of a Potent and Selective Sphingosine Kinase 1 Inhibitor through the Molecular Combination of Chemotype-Distinct Screening Hits. *J. Med. Chem.* **2017**, *60* (6), 2562−2572.
(30) Brown, P. D.; Willis, A. C.; Sherburn, M. S.; Lawrence, A. L. Total synthesis and structural revision of the alkaloid incargranine B. *Angew. Chem., Int. Ed.* **2013**, *52* (50), 13273−13275.
(31) Matto, P.; Modica, E.; Franchini, L.; Facciotti, F.; Mori, L.; de Libero, G.; Lombardi, G.; Fallarini, S.; Panza, L.; Compostella, F.; Ronchetti, F. A general and stereoselective route to alpha- or beta-galactosphingolipids via a common four-carbon building block. *J. Org. Chem.* **2007**, *72* (20), 7757−60.
(32) Schultz, V. L.; Zhang, X.; Linkens, K.; Rimel, J.; Green, D. E.; DeAngelis, P. L.; Linhardt, R. J. Chemoenzymatic Synthesis of 4-Fluoro-N-Acetylhexosamine Uridine Diphosphate Donors: Chain Terminators in Glycosaminoglycan Synthesis. *J. Org. Chem.* **2017**, *82* (4), 2243−2248.
(33) Ismaeel, A.; Kim, J. S.; Kirk, J. S.; Smith, R. S.; Bohannon, W. T.; Koutakis, P. Role of transforming growth factor-β in skeletal muscle fibrosis: a review. *Int. J. Mol. Sci.* **2019**, *20* (10), 2446.
(34) Zhang, F.; Xia, Y.; Yan, W.; Zhang, H.; Zhou, F.; Zhao, S.; Wang, W.; Zhu, D.; Xin, C.; Lee, Y.; Zhang, L.; He, Y.; Gao, E.; Tao, L. Sphingosine 1-phosphate signaling contributes to cardiac inflammation, dysfunction, and remodeling following myocardial infarction. *Am. J. Physiol Heart Circ Physiol* **2016**, *310*, H250−261.
(35) González-Fernández, B.; Sánchez, D. I.; Crespo, I.; San-Miguel, B.; Álvarez, M.; Tuñón, M. J.; González-Gallego, J. Inhibition of the SphK1/S1P signaling pathway by melatonin in mice with liver fibrosis and human hepatic stellate cells. *Biofactors* **2017**, *43*, 272−282.
(36) Ju, T.; Gao, D.; Fang, Z.-y. Targeting colorectal cancer cells by a novel sphingosine kinase 1 inhibitor PF-543. *Biochem. Biophys. Res. Commun.* **2016**, *470*, 728−734.
(37) Bond, M. R.; Zhang, H.; Vu, P. D.; Kohler, J. J. Photocrosslinking of glycoconjugates using metabolically incorporated diazirine-containing sugars. *Nat. Protoc.* **2009**, *4* (7), 1044−1063.
(38) Yablonka-Reuveni, Z.; Rivera, A. J. Proliferative dynamics and the role of FGF2 during myogenesis of rat satellite cells onisolatedfibers. *Basic Appl. Myol.* **1997**, *7*, 189−202.
(39) Leask, A.; Abraham, D. J. TGF-beta signaling and the fibrotic response. *FASEB J.* **2004**, *18* (7), 816−27.

https://dx.doi.org/10.1021/acsmedchemlett.9b00665
ACS Med. Chem. Lett. 2020, 11, 913−920